
Understanding Regularisation Methods for Continual Learning

Frederik Benzing

Department of Computer Science
 Institute of Theoretical Computer Science
 ETH Zurich
 8092 Zurich, Switzerland
 benzingf@inf.ethz.ch

Abstract

The problem of Catastrophic Forgetting has received a lot of attention in the past years. An important class of proposed solutions are so-called regularisation approaches, which protect weights from large changes according to their importances. Various ways to measure this importance have been put forward, all stemming from different theoretical or intuitive motivations. We present mathematical and empirical evidence that two of these methods – Synaptic Intelligence and Memory Aware Synapses – approximate a rescaled version of the Fisher Information, a theoretically justified importance measure also used in the literature. As part of our methods, we show that the importance approximation of Synaptic Intelligence is biased and that, in fact, this bias explains its performance best. Altogether, our results offer a theoretical account for the effectiveness of different regularisation approaches and uncover similarities between the methods proposed so far.

1 Introduction

Despite much progress, there remain many gaps between artificial and biological intelligence. Among these, the ability of animals to acquire new knowledge throughout their life has inspired a growing body of literature. In continual learning, a number of tasks are presented sequentially and the algorithm should learn new tasks without overwriting previous knowledge and without revisiting old data. An important class of algorithms proposed to solve this problem are regularisation approaches [21, 44, 3, 36, 6, 17, 37, 29]. They identify important weights after each task and protect them from large changes by modifying the loss function. At the heart of these algorithms lies the question how to estimate parameter importance, as this directly determines which parameters will be kept close to their old value and which parameters can be modified freely to solve new tasks. In this article, our aim is to understand why different importance measures proposed in the literature are effective. Notably, this question remains open for two well-known regularisation methods, Synaptic Intelligence (SI) [44] and Memory Aware Synapses (MAS) [3]. The latter approach has a purely heuristic motivation, while the former makes simplifying assumptions, violated in a deep learning setting, to theoretically justify its importance measure.

Our main contribution is to provide mathematical as well as empirical evidence that both these methods, SI and MAS, despite their different motivations, approximate a rescaled version of the Fisher Information. The Fisher Information has been used for continual learning [21] along with a clear theoretical, Bayesian justification [21, 17]. Thus, on top of unifying different regularisation-approaches proposed so far, our results give a more sound theoretical explanation for the effectiveness of two more continual learning algorithms.

To establish our claims, we first investigate MAS and give a simple mathematical derivation to show that MAS approximates what we call the Absolute Fisher. We carefully validate the assumptions of our derivations as well as the resulting claims empirically on standard continual learning benchmarks. As a second – maybe surprising – step we show that the importance approximation of SI is biased and that this bias contributes most to the continual learning performance of SI. Finally, we show that through this bias SI is – like MAS – closely related to the Absolute Fisher.

2 Related Work

Before reviewing the continual learning literature we point out that one of our algorithms is linked to the recently proposed Loss-Change-Allocation (LCA) [23]. This method gains insights into the training process of neural networks [2, 32, 39] by assessing how much the changes of individual parameters contribute to learning. To this end, LCA approximates the same path integral as Synaptic Intelligence [44]. For the approximation, the gradient has to be evaluated on the entire training set for each parameter update. Our method ‘Unbiased Synaptic Intelligence’ gives an unbiased estimate of the same quantity, but only using mini-batches, thus being computationally cheaper.

The problem of catastrophic forgetting in neural networks has been known and studied for many decades [28, 34, 12]. In the context of deep learning, it recently started receiving more attention again [15, 41]. An attempt to overcome this problem was made with the algorithm Elastic Weight Consolidation (EWC) [21]. We will review EWC and two other regularisation approaches – Synaptic Intelligence [44] and Memory Aware Synapses [3] – as well as their relatives [36, 6, 37] more closely in the next section. The idea of regularisation was also applied in the context of Bayesian neural networks in [29, 42], who use the weights’ posteriors after having learned a task as the prior for learning the next task.

On top of regularisation approaches, Parisi et al. [30] identify two more classes of continual learning approaches.

One of these classes are replay methods, which rely on data from old distributions to protect knowledge while learning new tasks. For example, iCarl [35] uses stored datapoints from old datasets and computes nearest neighbours in feature space for classification. GEM [26] and follow up work [7, 5] project gradients from new tasks onto directions that do not increase the loss on stored examples. However, empirical results from [8] suggest that one of the most effective ways to use small samples of old data is to simply mix them with the mini-batches of new data during training. To avoid storing old examples, which strictly speaking violates continual learning desiderata, *generative replay* methods train generative models to simulate old data distributions [38]. In this context, biologically inspired replay systems which mimic the hippocampus have also been put forward [19].

The third class of continual learning algorithms are architectural approaches, which use network expansion to learn new tasks without corrupting previous knowledge. PathNet [11] uses evolution to identify good subnetworks for each individual tasks, while [25] extends the network through neural architecture search. [37, 14] first train on a task, then compress the resulting net and iterate this process. Mixture models, with growing numbers of components, are investigated in [33, 24].

Finally, [43, 16, 10] point out that different continual learning scenarios and assumptions with varying difficulty were used across the literature. They also clearly define and distinguish these scenarios and test how well different algorithms perform in them.

3 Regularisation Methods for Continual Learning

In continual learning we are given K datasets $\mathcal{D}_1, \dots, \mathcal{D}_K$ sequentially. When training a neural net with N parameters $\theta \in \mathbb{R}^N$ on dataset \mathcal{D}_k , we have no access to the previously seen datasets $\mathcal{D}_{1:k-1}$ but should retain some memory of them. Regularisation based approaches introduced in [21, 17] do so by modifying the loss function L_k related to dataset \mathcal{D}_k . Let us denote the parameters obtained after finishing training on task k by $\theta^{(k)}$ and let $\Omega^{(k)}$ be some positive semi-definite $N \times N$ matrix. When training on task k , regularisation methods use the loss

$$\tilde{L}_k = L_k + c \cdot \left(\theta - \theta^{(k-1)} \right)^T \Omega^{(k-1)} \left(\theta - \theta^{(k-1)} \right). \quad (1)$$

where $c > 0$ is a hyperparameter. The first term in the loss function is the standard loss on task k . The second term makes sure that the parameters do not move away too far from the previous parameters.

It can already be seen that the matrix $\Omega^{(k)}$ can quickly become prohibitively large as it has N^2 entries, where N is the number of parameters. In practice, Ω is therefore often approximated by a diagonal matrix $\text{diag}(\omega_1, \dots, \omega_N)$. The loss function defined above then simplifies to

$$\tilde{L}_k = L_k + c \cdot \sum_{i=1}^N \omega_i^{(k-1)} \left(\theta_i - \theta_i^{(k-1)} \right)^2$$

and ω_i is often referred to as the importance of parameter θ_i . Usually, we have $\omega_i^{(k)} = \omega_i^{(k-1)} + \omega_i$, where ω_i is the importance for the most recently learned task k .

How good a regularisation based approach is, depends on how meaningful its importance estimates ω_i are. Different such estimates have been proposed and the aim of this work is to understand why different approaches work and how similar they are.

3.1 Detailed descriptions of algorithms

Broadly speaking (and to the best of our knowledge), three methods to measure parameter importance have been proposed, but see also below for adaptations of these methods.

Elastic Weight Consolidation [21] uses the diagonal of the Fisher Information as importance measure. It is evaluated at the end of training a given task. To define the *Fisher Information Matrix* F , let us assume we are given a dataset \mathcal{X} and that, for a datapoint X the network predicts a probability distribution (or equivalently, a vector of probabilities) \mathbf{q}_X with entries $\mathbf{q}_X(y)$ for $y \in L$, where L is the set of potential labels. Let us further assume that we use a categorical cross entropy loss $\text{CEL}(\mathbf{q}_X, y)$ and write $g(X, y) = \frac{\partial \text{CEL}(\mathbf{q}_X, y)}{\partial \theta}$ for its gradient.

Then the Fisher Information F is given as

$$F = \mathbb{E}_{X \sim \mathcal{X}} \mathbb{E}_{y \sim \mathbf{q}_X} [g(X, y)g(X, y)^T] \quad (2)$$

$$= \mathbb{E}_{X \sim \mathcal{X}} \sum_{y \in Y} \mathbf{q}_X(y) \cdot g(X, y)g(X, y)^T \quad (3)$$

Concretely, taking only the diagonal of F means

$$\omega_i(\text{EWC}) = \mathbb{E}_{X \sim \mathcal{X}} \mathbb{E}_{y \sim \mathbf{q}_X} [g_i(X, y)^2].$$

The *Empirical Fisher Information* matrix is an approximation of the Fisher Information, which rather than taking the expectation over $y \sim \mathbf{q}_X$ takes the (deterministic) label y given by the labels of the dataset. We will also define the *Predicted Fisher Information* as taking the maximum-likelihood predicted label, i.e. the argmax of $\mathbf{q}_X(y)$. Our empirical findings suggest that these different versions of the Fisher Information can be used almost exchangeably, see appendix.

The Fisher Information is often used as a measure of parameter sensitivity and under the assumption that the learned label distribution \mathbf{q}_X is the real label distribution it equals the Hessian of the loss (with respect to the real, not the empirical, label distribution) [27, 31]. Its effectiveness has a clean theoretical interpretation [21, 17].

Memory Aware Synapses [3] heuristically argues that the sensitivity of the final layer with respect to a parameter should be used as the parameter's importance. Similar to the Fisher Information, this sensitivity is evaluated after training a given task. Denoting, as before, the final layer of learned probabilities by \mathbf{q}_X , this means

$$\omega_i(\text{MAS}) = \mathbb{E}_{X \sim \mathcal{X}} \left[\left| \frac{\partial \|\mathbf{q}_X\|^2}{\partial \theta_i} \right| \right],$$

where the norm is Euclidean.¹

¹The authors of MAS point out that their measure could also be applied in an unsupervised setting, where the last layer does not necessarily represent predicted labels.

Synaptic Intelligence [44] approximates the contribution of each parameter to the decrease in loss and uses this contribution as importance. To formalise the ‘contribution of a parameter’, let us denote the parameters at time t by $\theta(t)$ and the loss by $L(t)$. If the parameters follow a smooth trajectory in parameter space, then we can write the *decrease* in loss between time 0 and T as

$$L(0) - L(T) = - \int_{\theta(0)}^{\theta(T)} \frac{\partial L(t)}{\partial \theta} \theta'(t) dt = - \sum_{i=1}^N \int_{\theta_i(0)}^{\theta_i(T)} \frac{\partial L(t)}{\partial \theta_i} \theta'_i(t) dt. \quad (4)$$

The i -th summand in (4) can be interpreted as the contribution of parameter i to the decrease in loss. While we cannot evaluate the integral precisely, we can use a first order approximation to obtain the importances. To do so, we write $\Delta_i(t) = (\theta_i(t+1) - \theta_i(t))$ for an approximation of $\theta'_i(t)dt$ and get

$$\tilde{\omega}_i(\text{SI}) = \sum_{t=0}^{T-1} \frac{\partial L(t)}{\partial \theta_i} \cdot \Delta_i(t).$$

In addition, SI rescales its importances as follows²

$$\omega_i(\text{SI}) = \frac{\max\{0, \tilde{\omega}_i(\text{SI})\}}{(\theta_i(T) - \theta_i(0))^2 + \xi}. \quad (5)$$

The authors of SI provide a theoretical argument for why this importance measure is equal to the Hessian of the loss under some assumptions. Not all of these assumptions seem realistic and we will show theoretically and empirically that the assumption of using full-batch-gradient-descent, which is violated in a deep-learning setting, has an important effect.

Related regularisation approaches. Strictly speaking, we presented a version of EWC described in [17] and tested in [6, 37]. Riemannian Walk [6] is a combination of EWC and a ‘KL-rescaled’ version of SI. Similar to EWC [36] uses the Fisher Information for regularisation, but rather than a diagonal approximation, finds a block diagonal approximation allowing to take layer-wise parameter interactions into account. While improving performance, this comes at the cost of a memory requirement of order $N \cdot K$ (where N is the number of parameters and K the number of tasks) which is enough memory to train and store separate networks for each task.³.

4 Theory & Methods

In this section we describe our theoretical motivations and design experiments to test our hypotheses, focussing on Memory Aware Synapses (MAS) in Section 4.1 and on Synaptic Intelligence (SI) in Section 4.2. The empirical results of our experiments will be presented in Section 5. An overview of different algorithms described here can be found in Table 1.

4.1 Memory Aware Synapses (MAS) and ‘Absolute Fisher Information’

We start by taking a closer look at the definition of the importances of MAS. We apply linearity of derivatives, the chain rule and write $y_0 = \arg \max \mathbf{q}_X$ to obtain

$$\frac{\partial \|\mathbf{q}_X\|^2}{\partial \theta} = 2 \sum_{y \in Y} \mathbf{q}_X(y) \frac{\partial \mathbf{q}_X(y)}{\partial \theta} \approx 2 \mathbf{q}_X(y_0) \frac{\partial \mathbf{q}_X(y_0)}{\partial \theta} = 2 \mathbf{q}_X^2(y_0) \frac{\partial \log \mathbf{q}_X(y_0)}{\partial \theta}. \quad (6)$$

Here we made the assumption that the sum is dominated by its maximum-likelihood label y_0 , which should be the case if the network classifies its images confidently, i.e. $\mathbf{q}(y_0) \gg \mathbf{q}(y)$ for $y \neq y_0$. Using the same heuristic for the Fisher Information we obtain

$$\mathbb{E}_{y \sim \mathbf{q}_X} [g(X, y)^2] \approx \mathbf{q}_X(y_0) g(X, y_0)^2.$$

Comparing this with (6) and recalling notation $g(X, y_0) = \partial \log \mathbf{q}_X(y_0)) / \partial \theta$, the similarity between MAS and the Fisher Information becomes apparent. The only difference is that MAS has an additional

²Note that the $\max(0, \cdot)$ is not part of the description in [44]. However, we needed to include it to reproduce their results. A similar mechanism can be found in the official SI code.

³This is especially relevant since the task-identity is usually known at test time for regularisation approaches.

Table 1: **Overview of different algorithms and their importance measures for one task.** Algorithms on the left calculate importance ‘online’ along the parameter trajectory during training. Algorithms on the right calculate importance at the end of training a task by going through (part of) the training set again. Correspondingly, the sum is over timesteps t (left) or datapoints X (right). N is the number of images over which is summed. Note that all the algorithms on the left rescale their final importances as in equation (5). In all algorithms $\Delta(t) = \theta(t+1) - \theta(t)$ refers to the parameter update at time t , which depends on both the current task’s loss and the regularisation loss. Moreover, $(g_t + \sigma_t)$ refers to the stochastic gradient estimate of the current task’s loss (where g_t is the full gradient and σ_t the noise) given to the optimizer (together with the regularisation loss) to calculate the parameter update. In contrast, $(g_t + \sigma'_t)$ refers to an independent stochastic gradient estimate of the current task loss. For a datapoint X , \mathbf{q}_X denotes the predicted label distribution and $g(X, y)$ refers to the gradient of datapoint X if it had label y .

Name	Parameter importance $\omega(\cdot)$	Name	Parameter importance $\omega(\cdot)$
SI	$\sum_t (g_t + \sigma_t) \Delta(t)$	Fisher	$\frac{1}{N} \sum_X \mathbb{E}_{y \sim \mathbf{q}_X} [g(X, y)^2]$
SIU (SI-Unbiased)	$\sum_t (g_t + \sigma'_t) \Delta(t)$	AF (Absolute Fisher)	$\frac{1}{N} \sum_X \mathbb{E}_{y \sim \mathbf{q}_X} [g(X, y)]$
SIB (SI Bias-only)	$\sum_t (\sigma_t - \sigma'_t) \Delta(t)$	MAS	$\frac{1}{N} \sum_X \left \frac{\partial \mathbf{q}_X ^2}{\partial \theta} \right $
OnAF (Online AF)	$\sum_t g_t + \sigma_t $	MASX (MAS-Max)	$\frac{1}{N} \sum_X \left \frac{\partial (\max \mathbf{q}_X)^2}{\partial \theta} \right $

factor of $2\mathbf{q}_X(y_0)$ and $g(X, y_0)$ is not squared. We therefore hypothesise that MAS is almost linearly dependent of the Absolute Fisher (AF), which is analogous to the Fisher Information, but takes absolute values of gradients rather than their squares, c.f. Table 1.

Our hypothesis is based on two assumptions: (1) The sum over the labels is dominated by its maximum likelihood label y_0 , cf. equation (6). (2) We assume that the factor $2\mathbf{q}_X(y_0)$ is roughly constant across most images X . To check (1), we explicitly evaluate the term of the sum based on y_0 (and call this $\omega(\text{MASX})$, see Table 1), and compare it to the entire sum (MASX vs MAS). Intuitively, (2) is justified because at the end of training most images X will have $q_X(y_0) \approx 1$. Note that even images with $q_X(y_0) = 0.5$ deviate only by a factor of 2, and still lead to a large correlation between MAS and AF. An empirical validation of (2) is checking if MASX and AF are linearly dependent. Both assumptions (1)&(2) are applicable in a wide range of settings, see Figures 2 (A) and 1b for strong empirical confirmations of them on standard benchmarks.

4.2 Synaptic Intelligence (SI)

4.2.1 Bias of Synaptic Intelligence

To calculate $\omega(\text{SI})$, we need to calculate the product $p = \frac{\partial L(t)}{\partial \theta} \cdot \Delta(t)$ at each step t . Since evaluating the full gradient $\frac{\partial L(t)}{\partial \theta}$ is prohibitively expensive, SI [44] uses a mini-batch. The resulting estimate is biased since the same mini-batch is used for the parameter update $\Delta(t)$ and the estimate of $\frac{\partial L(t)}{\partial \theta}$.

We now give the calculations detailing the argument above. For ease of exposition, let us assume that the network is optimized using vanilla SGD with learning rate 1. Given a mini-batch, denote its gradient estimate by $g + \sigma$, where $g = \frac{\partial L(t)}{\partial \theta}$ denotes the real gradient and σ the mini-batch noise. With SGD the parameter update equals $\Delta(t) = g + \sigma$. Thus, our product p should be $p = g \cdot (g + \sigma)$. However, using $g + \sigma$, which was used for the parameter update, to estimate $\frac{\partial L(t)}{\partial \theta_i}$ results in $p_{\text{biased}} = (g + \sigma)^2$. Thus, the gradient noise introduces a bias of $\mathbb{E}[\sigma^2 + \sigma g] = \mathbb{E}[\sigma^2]$.

Unbiased Synaptic Intelligence. It is easy to design an unbiased estimate of p by using two independent mini-batches to calculate the parameter update and to estimate g . This way we get $\Delta(t) = g + \sigma$ and an estimate $g + \sigma'$ for g from an independent mini-batch with independent noise σ' . We obtain $p_{\text{unbiased}} = (g + \sigma') \cdot (g + \sigma)$ which in expectation is equal to $p = g \cdot (g + \sigma)$. Based

on this we define an unbiased importance measure

$$\tilde{\omega}_i(\text{SIU}) = \sum_{t=0}^{T-1} (g_t + \sigma'_t) \cdot \Delta(t).$$

Bias-Only version of SI. To isolate the bias, we can simply take the difference between biased and unbiased estimate. Concretely, this gives a measure which only measures the bias of SI and is independent of the path integral,

$$\tilde{\omega}_i(\text{SIB}) = \sum_{t=0}^{T-1} ((g + \sigma) - (g + \sigma'_t)) \cdot \Delta(t).$$

Observe that this estimate multiplies the parameter-update $\Delta(t)$ with nothing but stochastic gradient noise. From the perspective of SI, this should not be meaningful and have poor continual learning performance.

Which part dominates SI? The approximations presented in equation (4) imply that $L(0) - L(T) \approx \sum_i \tilde{\omega}_i(\text{SI})$. Thus, comparing $\sum_i \tilde{\omega}_i$ for SI, SIU, SIB to $L(0) - L(T)$ measures how good the approximations are and shows whether SI is dominated by its bias, see Figure 1a. Further, comparing the continual learning performance of SI, SIU, SIB shows whether SI's continual learning performance relies on the approximation of the path integral or its bias, see Table 2, Exp No 2.

4.2.2 Synaptic Intelligence and Absolute Fisher Information

In this section we will indicate the relation between the importance measure $\omega(\text{SI})$ and the Fisher Information. Recall that $\omega(\text{SI})$ is a sum over terms $\frac{\partial L(t)}{\partial \theta} \cdot \Delta(t)$, where $\Delta(t) = \theta(t+1) - \theta(t)$ is the parameter update at time t . Recall as well that both terms in this product, $\frac{\partial L(t)}{\partial \theta}$ as well as $\Delta(t)$, are computed/approximated using the same mini-batch and thus the have the same noise.

For a precise understanding, we need to take into account how the optimizer uses stochastic gradients to update the parameters. In our experiments (as well as in the original SI experiments) we used the Adam optimizer [20]. Given a stochastic gradient $g_t + \sigma_t$, it keeps a running average of the gradient $m_t = (1 - \beta_1)(g_t + \sigma_t) + \beta_1 m_{t-1}$ as well as a running average of the squared gradients $v_t = (1 - \beta_2)(g_t + \sigma_t)^2 + \beta_2 v_{t-1}$. Ignoring some normalisation terms and the learning rate, the Adam parameter update is given by $\Delta(t) = m_t / (\sqrt{v_t} + \epsilon)$, where $\beta_1 = 0.9$ and $\beta_2 = 0.999$. Thus,

$$\frac{\partial L(t)}{\partial \theta} \Delta(t) = \frac{(1 - \beta_1)(g_t + \sigma_t)^2}{\sqrt{v_t} + \epsilon} + \frac{\beta_1(g_t + \sigma_t)m_{t-1}}{\sqrt{v_t} + \epsilon}.$$

Assuming that the noise σ_t is considerably bigger than the gradient g_t we obtain

$$\frac{\partial L(t)}{\partial \theta} \Delta(t) \approx (1 - \beta_1) \frac{(g_t + \sigma_t)^2}{\sqrt{v_t} + \epsilon} \quad (7)$$

The precise assumption made here is $(1 - \beta_1)\sigma_t^2 \gg \beta_1 m_{t-1} g_t$ (we ignore the term $\sigma_t m_{t-1}$ since $\mathbb{E}[\sigma_t m_{t-1}] = 0$ and since we average SI over many time steps). This assumption is supported strongly by Figure 1a, where the difference between green (SI) and blue (SIU) line is caused precisely by $(1 - \beta_1)\sigma_t^2$, see B.1 for full details. We also refer to [23] and Figures D.1, D.2 and F.5, F.4 for more evidence for the assumption that the noise is considerably bigger than the gradient.

Next, we consider v_t . It is a slowly moving average of $(g_t + \sigma_t)^2$ and will therefore be approximately $\mathbb{E}[(g_t + \sigma_t)^2]$. It is thus reasonable to expect that $\sqrt{v_t}$ is typically roughly proportional to $|g_t + \sigma_t|$. This clearly does not hold for all possible distributions of $g_t + \sigma_t$, but is unlikely to be violated by non adversarially chosen, realistic distributions. With (7) and $\sqrt{v_t} \approx |g_t + \sigma_t|$ we arrive at

$$\tilde{\omega}(\text{SI}) = \sum_t \frac{\partial L(t)}{\partial \theta} \Delta(t) \approx (1 - \beta_1) \sum_t \frac{(g_t + \sigma_t)^2}{\sqrt{v_t}} \approx \sum_t |g_t + \sigma_t|.$$

Our resulting approximation $\tilde{\omega}(\text{SI}) \approx \sum_t |g_t + \sigma_t|$ is very similar to the (Empirical) Absolute Fisher. The only differences are (1) the gradient in $\tilde{\omega}(\text{SI})$ is evaluated in mini-batches rather than on single

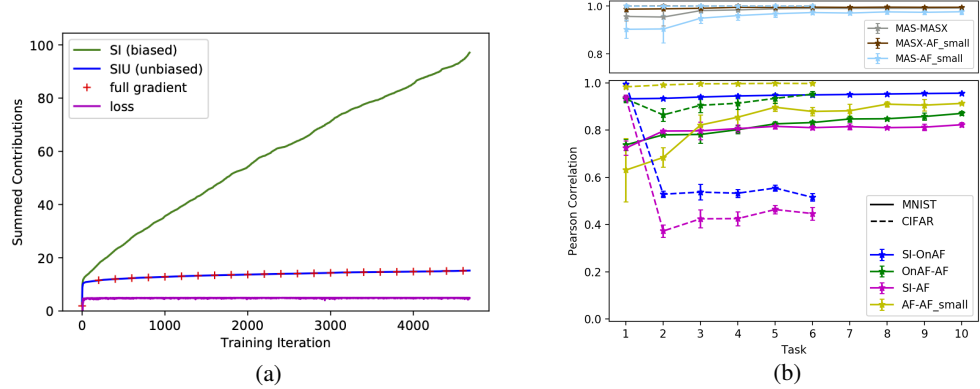


Figure 1: (a) **Summed importances** $\sum_i \tilde{\omega}_i$ for Permutated-MNIST. (b) **Pearson correlation for pairs of importance measures for all tasks.** Dashed lines represent CIFAR, solid lines MNIST. Error bars are stds across 4 runs. ‘AF’ is an estimate of the Absolute Fisher based on 30000 (MNIST) resp. 5000 (CIFAR) images. ‘AF_small’, ‘MAS’ and ‘MASX’ are based on 1000 resp. 500 images.

images; (2) the sum is taken ‘online’ along the parameter trajectory rather than at the final point of the trajectory. (1) does not have a large effect when $\sigma_t \gg g_t$ (as detailed in Appendix B.2) which is the case, c.f. our findings about gradient noise. The influence of (2) is hard to quantify theoretically and depends on how much the gradients change along the parameter trajectory. To capture this difference, we define the Online Absolute Fisher as $\tilde{\omega}(\text{OnAF}) = \sum_t |g + \sigma_t|$ and empirically test how similar $\tilde{\omega}(\text{OnAF})$ and $\tilde{\omega}(\text{AF})$ are.

Our heuristics suggest that $\tilde{\omega}(\text{SI})$ and $\tilde{\omega}(\text{OnAF})$ are very similar. If in addition, we empirically see that $\tilde{\omega}(\text{OnAF})$ and $\tilde{\omega}(\text{AF})$ are similar, this indicates that SI approximates AF, a rescaled version of the Fisher Information. Figures 2 and 1b empirically confirm both parts of this hypothesis.

We emphasise that our derivation above assumes that the parameter update $\Delta(t)$ is given by the gradients of the current task and ignores the regularisation term. The latter will change update direction and momentum of the optimizer. Thus, strong regularisation will make the relation between SI and OnAF noisy, but not abolish it. See Fig 1b (middle row) and Sec F.3 for confirmations hereof.

5 Experiments

In this section we empirically test our three main hypotheses:

1. Does Memory Aware Synapses approximate the Absolute Fisher as derived in Section 4.1?
2. Which part of the importance $\tilde{\omega}(\text{SI})$ of Synaptic Intelligence, the bias or the unbiased contribution, explains its effectiveness, see Section 4.2.1?
3. Does $\tilde{\omega}(\text{SI})$ indeed correlate strongly with the Absolute Fisher as indicated in Section 4.2.2?

5.1 Experimental Setup

Our experiments closely follow [44]. We use the **Permuted MNIST** [15] benchmark with 10 tasks, a fully connected ReLU architecture and a single output-head (‘domain incremental’ setting, c.f. [16, 43]) and the **Split CIFAR 10/100** benchmark with the keras default CNN and a multi-head output (‘task incremental’). Following [42], but unlike [44], we re-initialise model variables (fully connected layers, etc.) after each task and usually find better performance in our hyperparameter searchers. We defer further experimental details to the Appendix A. Code is available on github⁴.

5.2 Results

MAS and Absolute Fisher. Our first objective is to test whether MAS and Absolute Fisher are related. To this end we calculate $\omega(\text{MAS})$, $\omega(\text{MASX})$, $\omega(\text{AF})$ and show scatter plots of these values

⁴https://github.com/freedbee/continual_regularizer

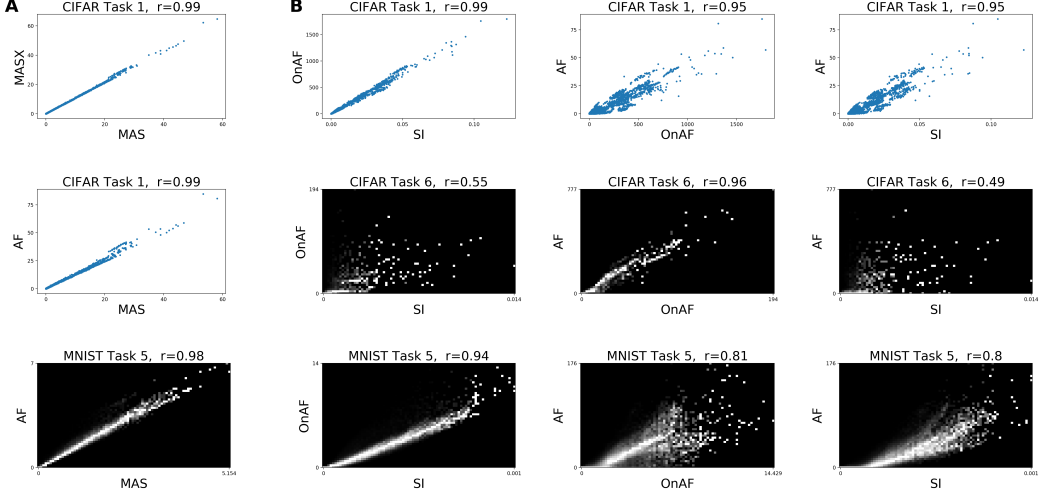


Figure 2: **Scatter- and Intensity plots for pairs of importance measures.** r denotes the Pearson correlation. *Scatter Plots (blue)*: Each point in the scatter plot corresponds to one weight of the net. A straight line through the origin corresponds to two importances measures being multiples of each other. *Intensity Plots (gray scale)*: Show data analogous to scatter plots, but are normalised for better visualisation. See Appendix A.1 for details and Figure F.6 for same data with only scatter/intensity plots. (A) Comparison between MAS, MASX, AF. (B) Comparison between SI, OnAF, AF on first task of CIFAR (top), last task of CIFAR (middle) and ‘middle’ task of MNIST (bottom).

in Figure 2 (A). We find that they are almost identical. Figure 1b shows equally strong correlations on the other tasks and datasets, presenting strong evidence for our heuristics. We also evaluated continual learning algorithms based on $\omega(\text{MAS})$, $\omega(\text{MASX})$, $\omega(\text{AF})$ and found very similar results, Table see 2, Exp No 1, providing further evidence that our mathematical derivations hold.

Why does SI work? To understand how large the bias of SI is, we track the sum $\sum_i \tilde{\omega}_i$ of importances for SI and its unbiased version SIU. As a control we include the decrease of the loss $L(0) - L(T)$ which the path-integral (c.f. equation (4)) approximates, as well as an first order approximation of the path-integral without relying on stochastic gradient estimates (computing the full training set gradient at each step). The results are portrayed in Figure 1a. They indicate that (1) the bias is 5-6 times larger than the unbiased part; (2) using an unbiased gradient estimate and using the entire training set gradient gives almost identical values of $\sum_i \omega_i$ supporting the validity of the unbiased estimator; (3) even the unbiased first order approximation of the path integral overestimates the decrease in loss. This is consistent with previous empirical studies showing that the loss has positive curvature [18, 23]. See Figures F.5, F.4 for similar results on CIFAR and other MNIST tasks.

We have seen that the SI’s bias is considerably larger than its unbiased component. This does not fully explain which of these parts is more essential for continual learning. We therefore run continual learning algorithms based on SI, its unbiased version (SIU) as well as a version which isolates the bias (SIB). The results are shown in Table 2, Exp No. 2. SIU consistently has worse performance than SI and SIB has the same or slightly better performance than SI. From SI’s perspective this is rather surprising and is convincing evidence that SI’s continual learning capability is due to its bias.

Is SI related to Absolute Fisher? Our main assumption in relating SI to Online Absolute Fisher (OnAF) was that the contribution of the noise (bias) to SI is bigger than its unbiased part, c.f. equation (7). We have already seen strong evidence that this is the case (Figure 1a). Therefore it may be expected that OnAF and SI do have significant correlations: On all tasks of MNIST and the first task of CIFAR, SI and OnAF have (Pearson) correlations > 0.93 ; on tasks 2-6 of CIFAR we find weaker, but significant correlations around 0.5, see Figures 2, 1b. This weaker correlation on CIFAR tasks 2-6 is well explained by regularisation, see 4.2.2 and Appendix F.3 for two control experiments.

Table 2: **Test accuracies on Permuted-MNIST and Split CIFAR 10/100.** Algorithms are grouped by experiment as indicated in main text. Reported results are mean and standard deviation over 3 resp. 10 runs for P-MNIST resp. CIFAR 10/100.

NO.	ALGO.	P-MNIST	CIFAR 10/100	NO.	ALGO.	P-MNIST	CIFAR 10/100
1	MAS	97.3 ± 0.1	73.7 ± 0.5	3	SI	97.2 ± 0.1	74.4 ± 0.5
	MASX	97.4 ± 0.2	73.7 ± 0.2		OnAF	97.3 ± 0.1	74.4 ± 0.6
	AF	97.4 ± 0.1	73.4 ± 0.4		AF	97.4 ± 0.1	73.4 ± 0.4
2	SI	97.2 ± 0.1	74.4 ± 0.5	4	EWC	97.2 ± 0.2	73.1 ± 0.7
	SIU	96.3 ± 0.1	72.5 ± 0.8		MAS	97.3 ± 0.1	73.7 ± 0.5
	SIB	97.2 ± 0.1	75.1 ± 0.4		AF	97.4 ± 0.1	73.4 ± 0.4

We also find that OnAF and AF are surprisingly similar, thus closely relating SI and AF (Figures 2, 1b) supporting our hypotheses.⁵ We also evaluate the corresponding continual learning algorithms SI, OnAF and AF, see Table 2, Exp 3. The results are very similar, indicating that SI, like MAS, works because it approximates a rescaled version of the Fisher Information.

Is Absolute or Real Fisher better for CL? We have seen evidence that both MAS and SI rely on estimating a rescaled Fisher Information. This raises the questions whether a rescaled version of the Fisher or the Fisher itself are more effective for continual learning. To answer this, we compare MAS, AF and EWC, since these methods all evaluate the importance at the end of training. The results are shown in Figure 2, Exp 4. All algorithms perform similarly, only the difference between MAS and EWC on CIFAR is significant ($p = 0.04$, t-test, not corrected for multiple comparisons). Which algorithm performs best may well depend on hyperparameters and the precise training set-up.

6 Relevance and Discussion

We have focused on regularisation approaches for continual learning and more specifically, how these methods assess parameter importance. We investigated three different importance measures proposed in the literature, namely Elastic Weight Consolidation, Synaptic Intelligence and Memory Aware Synapses. For standard (non-bayesian) neural networks these are (to the best of our knowledge) the only approaches to regularisation based continual learning. Other regularisation-related work directly relies on one of these algorithms or combinations of them [21, 44, 3, 4, 37, 36, 6, 17]. Originally, all three methods were motivated rather differently and suggested seemingly orthogonal importance measures. However, we gave heuristic mathematical derivations indicating that all methods nevertheless – and somewhat accidentally – are very closely related to the Fisher Information. We thoroughly checked the assumptions underlying our heuristics in realistic, standard continual learning set-ups and found convincing empirical support for our claims.⁶

On the one hand, our work unifies regularisation approaches proposed so far and highlights unexpected similarities. Our mathematical derivations do not only explain some surprising results, but also imply that our findings are more robust than merely observing empirical correlations.

On the other hand, our findings can have immediate practical consequences, as they help explain which algorithms are likely to work in which setting. There are several situations, in which we can make grounded predictions on the relative performance of MAS, SI and EWC. To be concrete, we exhibit how our insights may explain empirical observations presented in [9], which is an extensive comparative study of continual learning algorithms. (1) [9] finds that SI is sensitive to task-ordering when dataset sizes are imbalanced - namely, when small datasets are learned first SI overfits more. When training for a fixed number of epochs, small datasets will have small SI importances (since its biased sum contains few terms, independent of the path-integral) so that the net is subsequently less regularised and prone to overfit. (2) [9] notes that EWC suffers from having many weights with small

⁵ We check in F.1 that similarity of AF, OnAF does not depend on how long the networks are trained and show control correlations between SIU, SIB and (On)AF in F.2, further supporting our claim, that continual learning performance is explained by similarity to AF.

⁶The complexity of these set-ups and our limited understanding of neural networks in general mean that precise mathematical theorems quantifying when which methods are how similar are currently out of reach. We therefore believe that our simple, clear heuristics are more meaningful and instructive than theorems relying on unrealistic assumptions or only treating toy examples.

importances and performs worse than MAS. Note that relatively, MAS' (Absolute Fisher) rescaling makes small importances much bigger, explaining why it alleviates the small-importance problem. (3) [9] reports bad performance of SI in various settings. This may be due to learning rate decay, which gives more weight to early terms in SI's running sum. This makes the sum less related to the Fisher at the end of training, causing worse performance of SI. We note that (1) and (3) could be fixed by replacing SI by a normalised version of OnAF. We leave testing these hypotheses to future work and hope that our insights help developing, testing and improving regularisation methods.

Acknowledgements

I would like to thank Xun Zou, Florian Meier, Angelika Steger, Kalina Petrova and Asier Mujika for many helpful discussions and valuable feedback on this manuscript. I am also thankful for AM's technical advice and the Felix Weissenberger Foundation's ongoing support.

References

- [1] Martín Abadi, Paul Barham, Jianmin Chen, Zhifeng Chen, Andy Davis, Jeffrey Dean, Matthieu Devin, Sanjay Ghemawat, Geoffrey Irving, Michael Isard, et al. Tensorflow: A system for large-scale machine learning. In *12th {USENIX} Symposium on Operating Systems Design and Implementation ({OSDI} 16)*, pages 265–283, 2016.
- [2] Guillaume Alain and Yoshua Bengio. Understanding intermediate layers using linear classifier probes. *arXiv preprint arXiv:1610.01644*, 2016.
- [3] Rahaf Aljundi, Francesca Babiloni, Mohamed Elhoseiny, Marcus Rohrbach, and Tinne Tuytelaars. Memory aware synapses: Learning what (not) to forget. In *Proceedings of the European Conference on Computer Vision (ECCV)*, pages 139–154, 2018.
- [4] Rahaf Aljundi, Klaas Kelchtermans, and Tinne Tuytelaars. Task-free continual learning. In *Proceedings of the IEEE Conference on Computer Vision and Pattern Recognition*, pages 11254–11263, 2019.
- [5] Rahaf Aljundi, Min Lin, Baptiste Goujaud, and Yoshua Bengio. Gradient based sample selection for online continual learning. In *Advances in Neural Information Processing Systems*, pages 11816–11825, 2019.
- [6] Arslan Chaudhry, Puneet K Dokania, Thalaiyasingam Ajanthan, and Philip HS Torr. Riemannian walk for incremental learning: Understanding forgetting and intransigence. In *Proceedings of the European Conference on Computer Vision (ECCV)*, pages 532–547, 2018.
- [7] Arslan Chaudhry, Marc’ Aurelio Ranzato, Marcus Rohrbach, and Mohamed Elhoseiny. Efficient lifelong learning with a-gem. *arXiv preprint arXiv:1812.00420*, 2018.
- [8] Arslan Chaudhry, Marcus Rohrbach, Mohamed Elhoseiny, Thalaiyasingam Ajanthan, Puneet K Dokania, Philip HS Torr, and Marc’ Aurelio Ranzato. Continual learning with tiny episodic memories. *arXiv preprint arXiv:1902.10486*, 2019.
- [9] Matthias De Lange, Rahaf Aljundi, Marc Masana, Sarah Parisot, Xu Jia, Ales Leonardis, Gregory Slabaugh, and Tinne Tuytelaars. Continual learning: A comparative study on how to defy forgetting in classification tasks. *arXiv preprint arXiv:1909.08383*, 2019.
- [10] Sebastian Farquhar and Yarin Gal. Towards robust evaluations of continual learning. *arXiv preprint arXiv:1805.09733*, 2018.
- [11] Chrisantha Fernando, Dylan Banarse, Charles Blundell, Yori Zwols, David Ha, Andrei A Rusu, Alexander Pritzel, and Daan Wierstra. Pathnet: Evolution channels gradient descent in super neural networks. *arXiv preprint arXiv:1701.08734*, 2017.
- [12] Robert M French. Catastrophic forgetting in connectionist networks. *Trends in cognitive sciences*, 3(4):128–135, 1999.

- [13] Xavier Glorot and Yoshua Bengio. Understanding the difficulty of training deep feedforward neural networks. In *Proceedings of the thirteenth international conference on artificial intelligence and statistics*, pages 249–256, 2010.
- [14] Siavash Golkar, Michael Kagan, and Kyunghyun Cho. Continual learning via neural pruning. *arXiv preprint arXiv:1903.04476*, 2019.
- [15] Ian J Goodfellow, Mehdi Mirza, Da Xiao, Aaron Courville, and Yoshua Bengio. An empirical investigation of catastrophic forgetting in gradient-based neural networks. *arXiv preprint arXiv:1312.6211*, 2013.
- [16] Yen-Chang Hsu, Yen-Cheng Liu, Anita Ramasamy, and Zsolt Kira. Re-evaluating continual learning scenarios: A categorization and case for strong baselines. *arXiv preprint arXiv:1810.12488*, 2018.
- [17] Ferenc Huszár. Note on the quadratic penalties in elastic weight consolidation. *Proceedings of the National Academy of Sciences*, page 201717042, 2018.
- [18] Stanislaw Jastrzebski, Zachary Kenton, Nicolas Ballas, Asja Fischer, Yoshua Bengio, and Amos Storkey. On the relation between the sharpest directions of dnn loss and the sgd step length. *arXiv preprint arXiv:1807.05031*, 2018.
- [19] Ronald Kemker and Christopher Kanan. Farnet: Brain-inspired model for incremental learning. *arXiv preprint arXiv:1711.10563*, 2017.
- [20] Diederik P Kingma and Jimmy Ba. Adam: A method for stochastic optimization. *arXiv preprint arXiv:1412.6980*, 2014.
- [21] James Kirkpatrick, Razvan Pascanu, Neil Rabinowitz, Joel Veness, Guillaume Desjardins, Andrei A Rusu, Kieran Milan, John Quan, Tiago Ramalho, Agnieszka Grabska-Barwinska, et al. Overcoming catastrophic forgetting in neural networks. *Proceedings of the national academy of sciences*, 114(13):3521–3526, 2017.
- [22] Frederik Kunstner, Lukas Balles, and Philipp Hennig. Limitations of the empirical fisher approximation. *arXiv preprint arXiv:1905.12558*, 2019.
- [23] Janice Lan, Rosanne Liu, Hattie Zhou, and Jason Yosinski. Lca: Loss change allocation for neural network training. In *Advances in Neural Information Processing Systems*, pages 3614–3624, 2019.
- [24] Soochan Lee, Junsoo Ha, Dongsu Zhang, and Gunhee Kim. A neural dirichlet process mixture model for task-free continual learning. *arXiv preprint arXiv:2001.00689*, 2020.
- [25] Xilai Li, Yingbo Zhou, Tianfu Wu, Richard Socher, and Caiming Xiong. Learn to grow: A continual structure learning framework for overcoming catastrophic forgetting. *arXiv preprint arXiv:1904.00310*, 2019.
- [26] David Lopez-Paz and Marc’Aurelio Ranzato. Gradient episodic memory for continual learning. In *Advances in Neural Information Processing Systems*, pages 6467–6476, 2017.
- [27] James Martens. New insights and perspectives on the natural gradient method. *arXiv preprint arXiv:1412.1193*, 2014.
- [28] Michael McCloskey and Neal J. Cohen. Catastrophic interference in connectionist networks: The sequential learning problem. *Psychology of Learning and Motivation - Advances in Research and Theory*, 24(C):109–165, January 1989. ISSN 0079-7421. doi: 10.1016/S0079-7421(08)60536-8.
- [29] Cuong V Nguyen, Yingzhen Li, Thang D Bui, and Richard E Turner. Variational continual learning. *arXiv preprint arXiv:1710.10628*, 2017.
- [30] German I Parisi, Ronald Kemker, Jose L Part, Christopher Kanan, and Stefan Wermter. Continual lifelong learning with neural networks: A review. *Neural Networks*, 2019.

- [31] Razvan Pascanu and Yoshua Bengio. Revisiting natural gradient for deep networks. *arXiv preprint arXiv:1301.3584*, 2013.
- [32] Maithra Raghu, Justin Gilmer, Jason Yosinski, and Jascha Sohl-Dickstein. Svcca: Singular vector canonical correlation analysis for deep learning dynamics and interpretability. In *Advances in Neural Information Processing Systems*, pages 6076–6085, 2017.
- [33] Dushyant Rao, Francesco Visin, Andrei Rusu, Razvan Pascanu, Yee Whye Teh, and Raia Hadsell. Continual unsupervised representation learning. In *Advances in Neural Information Processing Systems*, pages 7645–7655, 2019.
- [34] Roger Ratcliff. Connectionist models of recognition memory: constraints imposed by learning and forgetting functions. *Psychological review*, 97(2):285, 1990.
- [35] Sylvestre-Alvise Rebuffi, Alexander Kolesnikov, Georg Sperl, and Christoph H Lampert. icarl: Incremental classifier and representation learning. In *Proceedings of the IEEE conference on Computer Vision and Pattern Recognition*, pages 2001–2010, 2017.
- [36] Hippolyt Ritter, Aleksandar Botev, and David Barber. Online structured laplace approximations for overcoming catastrophic forgetting. In *Advances in Neural Information Processing Systems*, pages 3738–3748, 2018.
- [37] Jonathan Schwarz, Jelena Luketina, Wojciech M Czarnecki, Agnieszka Grabska-Barwinska, Yee Whye Teh, Razvan Pascanu, and Raia Hadsell. Progress & compress: A scalable framework for continual learning. *arXiv preprint arXiv:1805.06370*, 2018.
- [38] Hanul Shin, Jung Kwon Lee, Jaehong Kim, and Jiwon Kim. Continual learning with deep generative replay. In *Advances in Neural Information Processing Systems*, pages 2990–2999, 2017.
- [39] Ravid Shwartz-Ziv and Naftali Tishby. Opening the black box of deep neural networks via information. *arXiv preprint arXiv:1703.00810*, 2017.
- [40] Nitish Srivastava, Geoffrey Hinton, Alex Krizhevsky, Ilya Sutskever, and Ruslan Salakhutdinov. Dropout: a simple way to prevent neural networks from overfitting. *The journal of machine learning research*, 15(1):1929–1958, 2014.
- [41] Rupesh K Srivastava, Jonathan Masci, Sohrob Kazerounian, Faustino Gomez, and Jürgen Schmidhuber. Compete to compute. In C. J. C. Burges, L. Bottou, M. Welling, Z. Ghahramani, and K. Q. Weinberger, editors, *Advances in Neural Information Processing Systems 26*, pages 2310–2318. Curran Associates, Inc., 2013. URL <http://papers.nips.cc/paper/5059-compete-to-compute.pdf>.
- [42] Siddharth Swaroop, Cuong V Nguyen, Thang D Bui, and Richard E Turner. Improving and understanding variational continual learning. *arXiv preprint arXiv:1905.02099*, 2019.
- [43] Gido M van de Ven and Andreas S Tolias. Three scenarios for continual learning. *arXiv preprint arXiv:1904.07734*, 2019.
- [44] Friedemann Zenke, Ben Poole, and Surya Ganguli. Continual learning through synaptic intelligence. In *Proceedings of the 34th International Conference on Machine Learning-Volume 70*, pages 3987–3995. JMLR. org, 2017.

APPENDIX

This appendix has several components:

1. We give full experimental details including hyperparameter seraches and values in Section A.
2. We give the details of two calculations omiited in our derivation that SI and AF are related, see B
3. We describe some variants of SI and OnAF, which we tried with the aim of improving performance in Section C.
4. We empirically investigate the gradient noise in Section D. This experiment is not specific to continual learning.
5. We provide an empirical comparison of different versions of the Fisher Information ('real', 'empirical' and 'predicted') in Section E.
6. We include additional experiments and some additional plots in Section F.

A Experimental details

We tried to include all details necessary to reproduce our results here. If we forgot something, don't hesitate to send us an email. Code will also be available on [github](#).

A.1 Scatter Plot Data Collection and Intensity Plots

The scatter plots in Figure 2 are based on a run of SI, where we in parallel to evaluating the SI importance measure also evaluated all other importance measures. AF is evaluated using 30000 samples on MNIST and 500 on CIFAR. Figure 1b shows data based on 4 repetitions of this experiment and confirms that the correlations observed in the scatter plots are representative, it also shows the effect of sample sizes on AF. In addition, we gathered data following the precise setup of [44], i.e. without reinitialising model variables after each task, and found even stronger support for our heuristics in this setting, see Section F.3.

Intensity Plots Show same kind of data as scatter plots, but each weight is binned into one of 80x50 equispaced bins. The number of weights per bin is divided by the maximum number of weights per bin in that column and the resulting value is shown on a gray scale. Normalisation per column was performed as for 'global normalisation' only weights in the bottom left are visible; the number of bins was chosen to match aspect ratio of plots.

A.2 Benchmarks

In **Permuted MNIST** [15] each task consists of predicting the label of a random (but fixed) pixel-permutation of MNIST. We use a total of 10 tasks. As noted, we use a domain incremental setting, i.e. a single output head shared by all tasks.

In **Split CIFAR10/100** the network first has to classify CIFAR10 and then is successively given groups of 10 (consecutive) classes of CIFAR100. As in [44], we use 6 tasks in total. Preliminary experiments on the maximum of 11 tasks showed very little difference. We use a task-incremental setting, i.e. each task has its output head and task-identity is known during training and testing.

A.3 Pre-processing

Following [44], we normalise all pixel values to be in the interval $[0, 1]$ (i.e. we divide by 255) for MNIST and CIFAR datasets and use no data augmentation. We point out that pre-processing can affect performance, e.g. differences in pre-processing are part of the reason why results for SI on Permuted-MNIST in [16] are considerably worse than reported in [44] (the other two reasons being an unusually small learning rate of 10^{-4} for Adam in [16] and a slightly smaller architecture).

A.4 Architectures and Initialization

For P-MNIST we use a fully connected net with ReLu activations and two hidden layers of 2000 units each. For Split CIFAR10/100 we use the default Keras CNN for CIFAR 10 with 4 convolutional layers and two fully connected layers, dropout [40] and maxpooling, see Table A.1. We use Glorot-uniform [13] initialization for both architectures.

A.5 Optimization

We use the Adam Optimizer [20] with tensorflow [1] default settings ($lr = 0.001, \beta_1 = 0.9, \beta_2 = 0.999, \epsilon = 10^{-8}$) and batchsize 256 for both tasks like [44]. We reset the optimizer variables (momentum and such) after each task.

A.6 SI & OnAF details

Recall that we applied the operation $\max(0, \cdot)$ (i.e. a ReLU activation) to the importance measure of each individual task (equation (5) of main paper), before adding it to the overall importance. In the original SI implementation, this seems to be replaced by applying the same operation to the overall importances (after adding potentially negative values from a given task). No description of either of these operations is given in the SI-paper. In light of our findings, our version seems more justified.

Somewhat naturally, the gradient $\frac{\partial L}{\partial \theta}$ usually refers to the cross-entropy loss of the current task and not the total loss including regularisation. For CIFAR we evaluated this gradient without dropout (but the parameter update was of course evaluated with dropout).⁷

For OnAF, similarly to SI, we used the gradient evaluated without dropout on the cross-entropy loss of the current task for our importance measure.

A.7 Estimating Fisher Information, MAS, etc.

When estimating Fisher Information / MAS, we do not iterate over the whole training set, due to the considerable computational cost. We sample uniformly random subsets of size 1000 (P-MNIST) and 500 (CIFAR). In preliminary experiments with twice as large subsets we found no improvement in average accuracy. When comparing two different measures (e.g. MAS and AF) we use the same samples to calculate both measures to avoid unnecessary noise in our comparisons.

Table A.1: CIFAR 10/100 architecture. Following [44] we use the keras default architecture for CIFAR 10. Below, ‘Filt.’ refers to the number of filters of a convolutional layer, or respectively the number of neurons in a fully connected layer. ‘Drop.’ refers to the dropout rate. ‘Non-Lin.’ refers to the type of non-linearity used.

Table reproduced and slightly adapted from [44].

Layer	Kernel	Stride	Filt.	Drop.	Non-Lin.
3x32x32 input					
Convolution	3x3	1x1	32		ReLU
Convolution	3x3	1x1	32		ReLU
MaxPool	2x2	2x2		0.25	
Convolution	3x3	1x1	64		ReLU
Convolution	3x3	1x1	64		ReLU
MaxPool	2x2	2x2		0.25	
FC			512	0.5	ReLU
Task 1: FC			10		softmax
...:FC			10		softmax
Task 6: FC			10		softmax

⁷We did not check the original SI code for what’s done there and the paper does not describe which version is used.

Table A.2: Hyperparameter values for our experiments. See also maintext.

Algorithm	MNIST		CIFAR	
	c	re-init	c	re-init
SI	0.2	✓	5.0	✓
SIU	2.0	✓	2.0	✗
SIB	0.5	✓	5.0	✓
OnAF	5e-5	✓	5e-4	✓
MAS	500	✗	200	✓
MASX	200	✗	1e3	✓
EWC	5e3	✗	5e4	✓
AF	200	✗	5e4	✓

A.8 Hyperparameters

For all methods and benchmarks, we performed grid searches for the hyperparameter c and over the choice whether or not to re-initialise model variables after each task.

The grid of c included values $a \cdot 10^i$ where $a \in \{1, 2, 5\}$ and i was chosen in a suitable range (if a hyperparameter close to a boundary of our grid performed best, we extended the grid).

For CIFAR, we measured validation set performance based on at least three repetitions for good hyperparameters. We then picked the best HP and ran 10 repetitions on the test set. For MNIST, we measured HP-quality on the test set based on at least 3 runs for good HPs.

Additionally, SI and consequently SIU, SIB as well as OnAF have rescaled importance (c.f. equation (5) from main paper). The damping term ξ in this rescaling was set to 0.1 for MNIST and to 0.001 for CIFAR following [44] without further HP search.

All results shown are based on the same hyperparameters obtained – individually for each method – as described above. They can be found in Table A.2. We note that the difference between the HPs for MAS and MASX might seem to contradict our claims that the two measures are almost identical (they should require the same c in this case), but this is most likely due to similar performance for different HPs and random fluctuations. For example on CIFAR, MAS had almost identical validation performance for $c = 200$ (best for MAS) and $c = 1000$ (best for MASX) (74.2 ± 0.7 vs 74.1 ± 0.5).

Also for the other methods, we observed that usually there were two or more HP-configurations which performed very similarly. The precise ‘best’ values as found by the HP search and reported in Table A.2 are therefore subject to random fluctuations in the grid search.

B Two Calculations

Here we give two calculations omitted Secontion 4.2.2 of the main paper.

B.1 Bias of SI with Adam

We claimed that the difference between SI and SIU (green and blue line) seen in Figure 1a (and also in Figures F.4, F.5) is due to the term $(1 - \beta_1)\sigma_t^2$. To see this, recall that for SI, we approximate $\frac{\partial L(t)}{\partial \theta}$ by $g_t + \sigma_t$, which is the same gradient estimate given to Adam. So we get

$$\text{SI: } \frac{\partial L(t)}{\partial \theta} \Delta(t) = \frac{(1 - \beta_1)(g_t + \sigma_t)^2}{\sqrt{v_t + \epsilon}} + \frac{\beta_1(g_t + \sigma_t)m_{t-1}}{\sqrt{v_t + \epsilon}}.$$

For SIU, we use an independent mini-batch estimate $g_t + \sigma'_t$ for $\frac{\partial L(t)}{\partial \theta}$ and therefore obtain

$$\text{SIU: } \frac{\partial L(t)}{\partial \theta} \Delta(t) = \frac{(1 - \beta_1)(g_t + \sigma'_t)(g_t + \sigma_t)}{\sqrt{v_t + \epsilon}} + \frac{\beta_1(g_t + \sigma'_t)m_{t-1}}{\sqrt{v_t + \epsilon}}.$$

Taking the difference between these two and ignoring all terms which have expectation zero (note that $\mathbb{E}[\sigma_t] = \mathbb{E}[\sigma'_t] = 0$ and that σ_t, σ'_t are independent of m_{t-1} and g_t) gives

$$\text{SI} - \text{SIU: } (1 - \beta_1) \frac{\sigma_t^2}{\sqrt{v_t + \epsilon}}$$

as claimed.

Note also that in expectation SIU equals $(1 - \beta_1) \frac{g_t^2}{\sqrt{v_t + \epsilon}} + \beta_1 \frac{g_t m_{t-1}}{\sqrt{v_t + \epsilon}}$ so that a large difference between SI and SIU really means $(1 - \beta_1)\sigma_t^2 \gg (1 - \beta_1)g_t^2 + \beta_1 m_{t-1}g_t \approx \beta_1 m_{t-1}g_t$. The last approximation here is valid because $\beta_1 m_{t-1} \gg (1 - \beta_1)g_t$ which holds since (1) $\beta_1 \gg (1 - \beta_1)$ and (2) we have $\mathbb{E}[m_{t-1}] \approx g_t$ and m_{t-1} additionally has a noise component, which g_t does not have, so that $\mathbb{E}[|m_{t-1}|] > \mathbb{E}[|g_t|]$.

B.2 Effect of Calculating Fisher in Batches

For this subsection, let us slightly change notation and denote the images by X_1, \dots, X_D and the gradients (with respect to their labels and the cross entropy loss) by $g + \sigma_1, \dots, g + \sigma_D$. Here, again g is the overall training set gradient and σ_i is the noise (i.e. $\sum_{i=1}^D \sigma_i = 0$). Then the Empirical Fisher is given by

$$\text{EF} = \frac{1}{D} \sum_{i=1}^D (g + \sigma_i^2)$$

We want to compare this to evaluating the squared gradient over a batch. Let i_1, \dots, i_b denote uniformly random, independent indices from $\{1, \dots, D\}$, so that X_{i_1}, \dots, X_{i_b} is a random mini-batch of size b . Let $g + \sigma$ be the gradient on this mini-batch. We then have, taking expectations over the random indices,

$$\begin{aligned} \mathbb{E}[(g + \sigma)^2] &= \mathbb{E} \left[\frac{1}{b^2} \sum_{r,s=1}^b (g + \sigma_{i_r})(g + \sigma_{i_s}) \right] \\ &= \frac{b(b-1)}{b^2} \mathbb{E}[(g + \sigma_{i_1})(g + \sigma_{i_2})] + \frac{b}{b^2} \mathbb{E}[(g + \sigma_{i_1})^2] \\ &= \frac{b-1}{b} g^2 + \frac{1}{b} \text{EF} \\ &\approx \frac{1}{b} \text{EF} \end{aligned}$$

This conclusion may seem surprising, but please recall that it is only based on one assumption, namely that the gradient noise is considerably bigger than the gradient itself - an assumption for which we have collected ample evidence.

Concretely, we assume $\mathbb{E}[(g + \sigma)^2] \gg (b-1)g^2$. Note that unlike in other sections of this manuscript, here σ refers to the gradient noise of individual images (rather than mini-batch noise). We have seen that even with a batch-size of 256 (i.e. when we reduce the noise by a factor of 256) the noise is still much bigger than the gradient (recall one more time Figures F.4, F.5, D.1, D.2), so that our assumption is true with room to spare.

We also mention preliminary and rather unsurprising experiments, in which we evaluated the Empirical Fisher in mini-batches on P-MNIST (at the end of training a task) and observed the same performance as when evaluating the Empirical Fisher (and also ‘real’ Fisher, for that matter) on single images.

C Variants of SI/OnAF

Based on our findings, we tried several adoptions of SI as described below.

Firstly, rather than taking the running sum of the product of gradient and update for SI, we experimented with an exponential moving average (EMA). We tried this based on our evidence that SI approximates some form of the Fisher Information. The EMA puts more weight on recently observed samples of this value, which should be more related to the actual Fisher Information and discards information which stems too far from the past. We performed HP searches over different decay factors for the running average on P-MNIST and found small improvements. Additionally, we found that the EMA is less stable if training time is increased (to e.g. 100 or 200 epochs per task). In this case, the magnitude of the EMA after for example the first task varies greatly from run to run (since

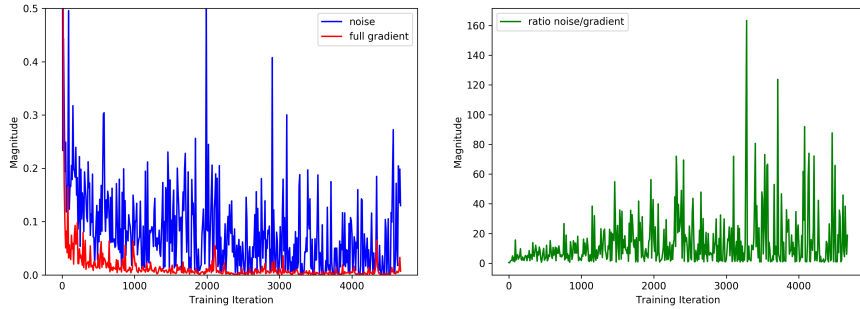


Figure D.1: Gradient noise, measured as squared ℓ_2 distance between full training set gradient and the stochastic mini-batch gradient with a batch size of 256. ‘Full gradient’ magnitude is also measured as squared ℓ_2 norm.

Data obtained by training a ReLu network with 2 hidden layers of 2000 hidden units for 20 epochs with default Adam settings. Only every 20-th datapoint shown for better visualisation.

the parameters may or may not be in a very flat region of the loss landscape), while the running sum (as in SI) is more stable (as we observed empirically).

Secondly, observe that the magnitude of the per-task-importance of SI depends largely on how long we train, rather than on the change in loss. This can be seen for examples in Figure F.5, where the importances of the CIFAR 100 tasks are considerably smaller than the importance of the CIFAR 10 task. This is partly because each class in CIFAR 100 has 10 times less training samples, corresponding to 10 times less training iterations when keeping the number of epochs fixed (at 60 in our case). This suggests rescaling the per-task-importance by the number of training iterations of that task. We simply divided the importance of each task by the number of training iterations of that task (and performed a new HP search). We found no change in performance with this rescaling.

Thirdly, recall that we argued that SI is closely related to the running sum of absolute gradient values, OnAF. We also implemented an importance measure based on the running sum of squared gradients (OnF – Online Fisher), as this variant more closely matches the Real Fisher Information. We observed a slight decrease in performance.

We believe that our findings may indicate that regularisation based continual learning is fairly robust to rescaling its importance measures, at least on the datasets/settings we tested.

D Gradient Noise

Here, we quantitatively assess the noise magnitude outside the continual learning context. Recall that Figure 1a from the main paper, as well as Figures F.4 and F.5 already show that the noise dominates the SI importance measure, which indicates that the noise is considerably larger than the gradient itself.

To obtain an assessment independent of the SI continual learning importance measure, we trained our network on MNIST as described before, i.e. a ReLu network with 2 hidden layers of 2000 units each, trained for 20 epochs with batch size 256 and default Adam settings. At each training iteration, on top of calculating the stochastic mini-batch gradient used for optimization, we also computed the full gradient on the entire training set and computed the noise – which refers to the squared ℓ_2 distance between the stochastic mini-batch gradient and the full gradient – as well as the ratio between noise and gradient, measured as the ratio of squared ℓ_2 norms. The results are shown in Figure D.1. In addition, we computed the fraction of iterations in which the ratio between noise and squared gradient norm is above a certain threshold, see Figure D.2.

E Comparison of different variants of Fisher Information

It is not fully clear which version of Fisher Information is used for EWC and its variants, since ‘Empirical’ and ‘Real’ Fisher Information are both often referred to simply as ‘Fisher Information’ in

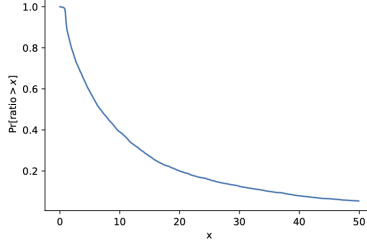


Figure D.2: y -value shows fraction of training iterations in which the ratio between mini-batch noise and full training set gradient was at least x -value. Data obtained as described in main text / Figure D.1, in particular the batch-size was 256. ‘Ratio’ refers to the ratio of squared ℓ_2 norms of the respective values.

the literature. Neither [21] nor [37] make code available, or provide details in the description of their algorithms.

We compare different variants here and note that [43] also hints at such a comparison. We compare ‘empirical’, ‘predicted’ as well as ‘real’ Fisher, as described in the main paper. Note that, at least with a naïve implementation, the real Fisher takes 10 times longer to compute than empirical and predicted Fisher, where 10 is the number of potential output labels. More efficient ways to calculate the Fisher Information [22, 27] are not directly supported by standard deep learning libraries (at the time of writing, to the best of our knowledge).

We report continual learning performance based on the different Fisher Informations in Table E.1 and find very little difference.

Additionally, we trained SI on P-MNIST and Split CIFAR and evaluated the different kinds of Fisher at the end of each task using the same samples of the training set (10 tasks for P-MNIST and 6 tasks for CIFAR) and calculated the Pearson Correlations.

For real and empirical Fisher, on P-MNIST the correlation was between 0.49 and 0.91; on Split CIFAR it was between 0.77 and 0.99.

For real and predicted Fisher, on P-MNIST the correlation was between 0.75 and 0.92; on Split CIFAR it was between 0.77 and 1.00.

Table E.1: Classification accuracies for different versions of Fisher Information evaluated on Permuted-MNIST and Split CIFAR 10/100.

ALGORITHM	P-MNIST	CIFAR 10/100
REAL FISHER (EWC?)	97.2 ± 0.2	73.1 ± 0.7
EMPIRICAL FISHER	97.0 ± 0.1	73.0 ± 0.5
PREDICTED FISHER	97.1 ± 0.1	72.9 ± 0.8

F More Experiments and Plots

For SI, we note that the observation that most of the SI importance is due to its bias is consistent across datasets and tasks, see Figures F.4 and F.5. Intriguingly, on CIFAR we find that the unbiased approximation of SI slightly underestimates the decrease in loss in the last task, suggesting that strong regularisation pushes the parameters in places, where the cross-entropy of the current task has negative curvature.

We show analogues of Figure 2 consisting of only scatter/ only intensity plots in Figure F.6. Note that for both architectures there are a few million weights. The scatter plots are overcrowded and show the whole range of dependencies between two measure that can possibly occur. Intensity plots show the dependencies that the majority of weights adheres to.

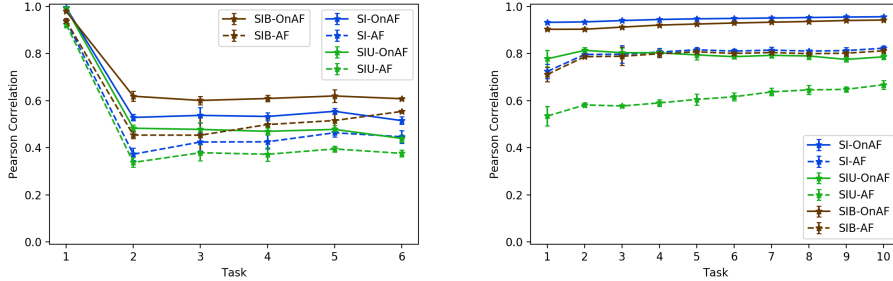


Figure F.1: Analogous to Figure 1b from main paper, comparing SI, SIU, SIB. Left: CIFAR, Right: MNIST

F.1 Influence of Training Duration on AF, OnAF

It seems plausible that the correlation between AF and OnAF we observed is due to training on tasks for a long time – the model might converge quickly so that the sum of OnAF is dominated by summands which approximate AF close to the final point in training. To test this, we trained our networks for varying numbers of epochs on the first task of P-MNIST and Split CIFAR10/100 and measured the correlation between OnAF and AF. The results in Tables F.1, F.2 show that the correlation between AF, OnAF does not rely on long training duration. On MNIST, we even see decreasing correlation with longer training time, this may be due to either an actual decrease in correlation or due to higher variance when estimating AF using 10000 samples (or both).

Table F.1: **Correlation between AF and OnAF on CIFAR10 depending on training time.** We show mean and standard deviation of Pearson correlation over 3 runs. AF is based on 500 samples. If the standard deviation is below 0.005 it is shown as 0.00.

NUMBER OF EPOCHS	CORRELATION
1	0.94± 0.01
2	0.95± 0.00
4	0.96± 0.01
8	0.96± 0.01
15	0.97± 0.00
30	0.97± 0.00
60	0.95± 0.01

Table F.2: **Correlation between AF and OnAF on MNIST depending on training time.** We show mean and standard deviation of Pearson correlation over 3 runs. AF is based on 10000 samples.

NUMBER OF EPOCHS	CORRELATION
1	0.90± 0.01
2	0.90± 0.01
5	0.88± 0.01
10	0.78± 0.04
20	0.68± 0.05

F.2 Comparisons between SI, SIU and SIB

Here, we show correlations of SIU, SIB with OnAF, AF as controls, see Figure F.1. We generally find that SIU is less correlated with AF/OnAF than SI, SIB as predicted by our heuristic derivations. This is in line with our hypothesis that performance of these algorithms is largely explained by their relation to (On)AF.

The only exception is the first task of CIFAR (i.e. CIFAR10), where correlation with OnAF is 0.994 ± 0.001 for SI; 0.991 ± 0.001 for SIU; 0.979 ± 0.003 for SIB. The similarity between SIU and OnAF in this situation is explained by the weights with largest OnAF importance: If we remove the 5% of weights which have highest OnAF importance, correlation between OnAF, SIU drops to 0.599 ± 0.027 , but for SI resp. SIB the same procedure yields 0.977 ± 0.002 resp. 0.965 ± 0.003 . This indicates that for the first task of CIFAR there is a small fraction of weights with large OnAF importances, which are dominated by the gradient rather than the noise. The remainder of weights is in accordance with our previous observations and dominated by noise, recall also Figure F.5.

F.3 Effect of regularisation on SI

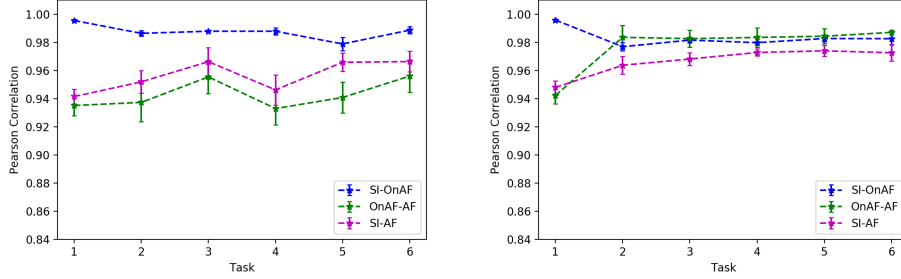


Figure F.2: Note y-scale. Analogous to Figure 1b from main paper, showing data from CIFAR and confirming that with weaker regularisation, OnAF and SI are similar. Left: Showing runs of SI with $c = 0$. Right: Showing runs of SI without reinitialising network weights.

We perform two experiments to check whether the weaker correspondence between SI, OnAF on CIFAR tasks 2-6 as compared to CIFAR task1 is really due to regularisation. Firstly, we set the hyperparameter c governing the strength of regularisation to 0. We show results in Figure F.2, finding that correspondence is as strong on tasks 2-6 as it was on the first task. Secondly, we precisely follow the setting of the original SI method [44] and do not reinitialize the network weights after each task. Note that in this setting, the optimal hyper parameter as found by our HP search is $c = 0.5$ and validation performance is slightly worse (72.4 ± 1.0 without re-initialisation vs 74.9 ± 0.6 with reinitialisation and $c = 0.5$). In addition to smaller c , the lack of reinitialisation means that the parameters will never get too far away from the optimum of the old task during optimization, meaning that the regularisation-gradients are smaller. Indeed, we find that in this case there is a strong correspondence between OnAF and SI as shown in Figure F.2.

Finally, we point out that our comparisons are usually obtained after applying a $\max(0, \cdot)$ (c.f. equation (5) of main paper) to the SI (and SIU, SIB) importances as the algorithms diverge without this operation. We present results without this max operation in F.3, further showing that (1) correlation between OnAF and SI is weakened by strong regularisation and (2) the correlation is due to the bias of SI. See also Figure F.7.

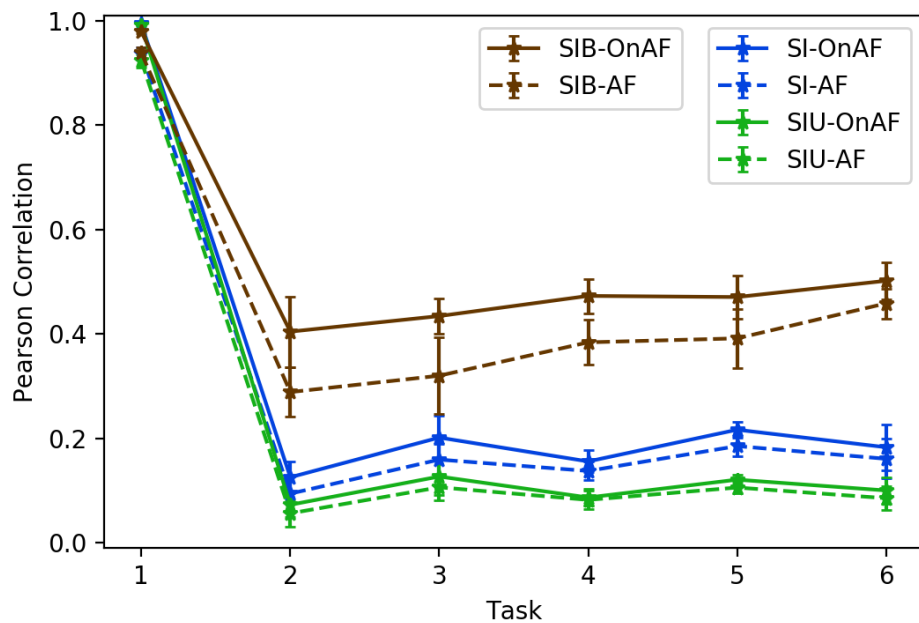


Figure F.3: Analogous to Figure 1b from main paper, comparing SI, SIU, SIB but before the operation $\max(\cdot, 0)$ is applied to importances of SI, SIU, SIB. See fulltext.

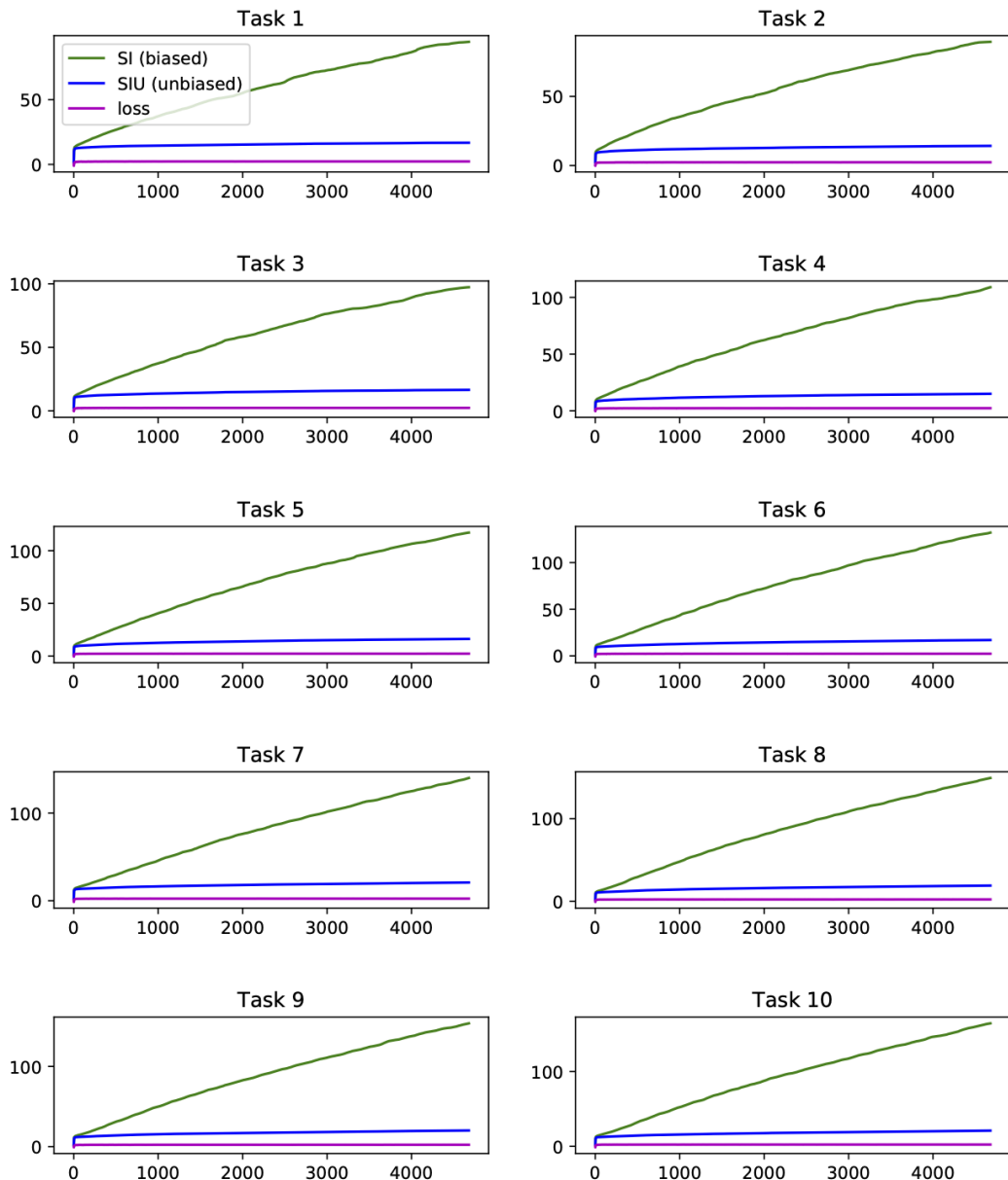


Figure F.4: Summed importances for all P-MNIST tasks for SI and its unbiased version. Analogous to Figure 1a from main paper.

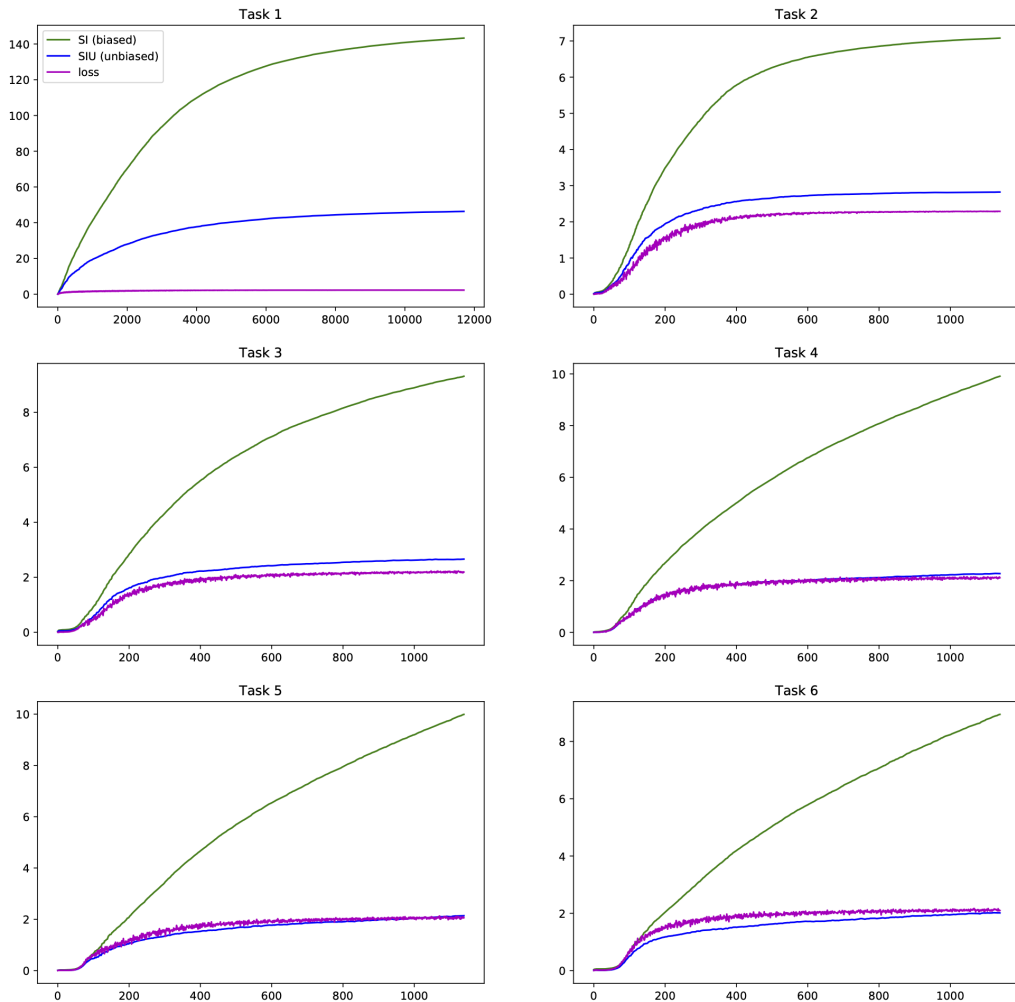


Figure F.5: Summed importances for all Split CIFAR 10/100 tasks for SI and its unbiased version..
Analogous to Figure 1a from main paper.

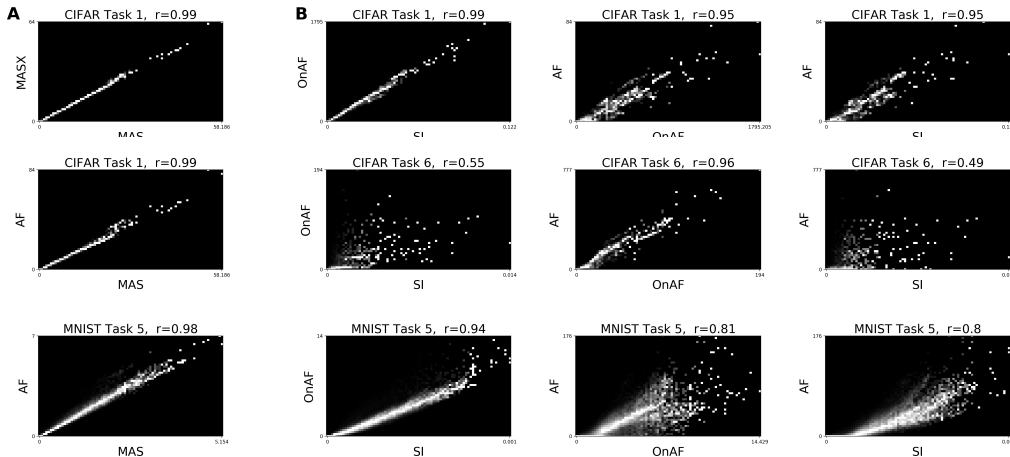
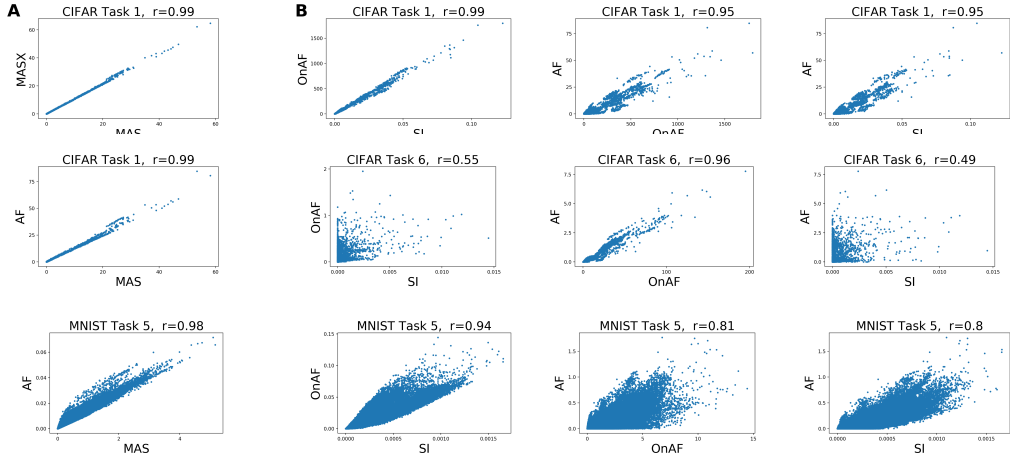


Figure F.6: Same data as Figure 2 from main paper.

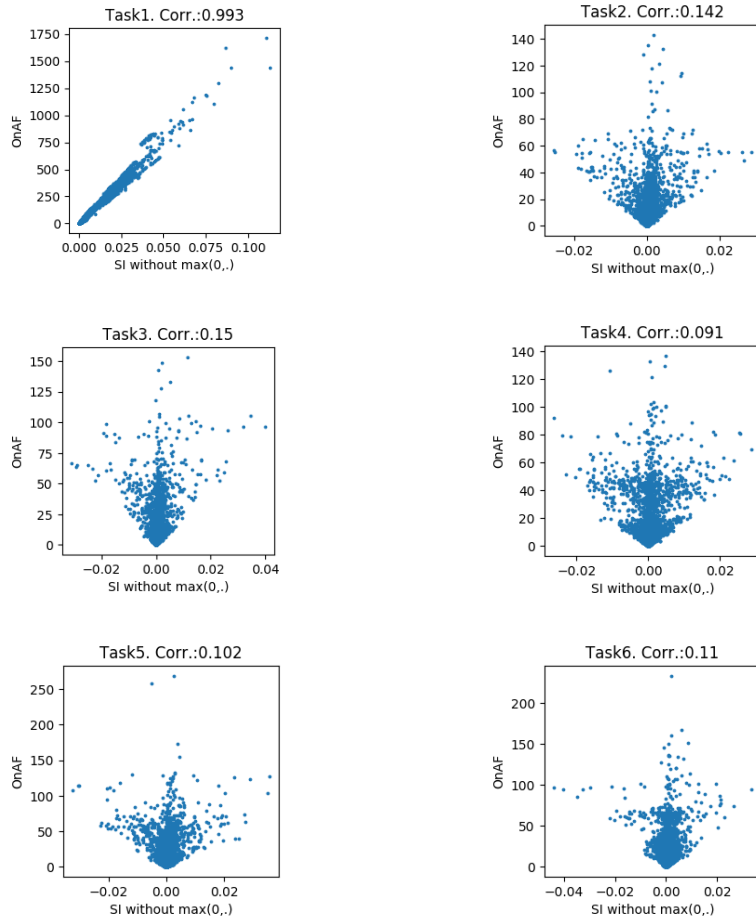


Figure F.7: Scatter plots of a variant of SI, which does not set negative per-task-importances to 0 after each task. Refer to main text for more details, see also Figure F.3

References

- [1] Martín Abadi, Paul Barham, Jianmin Chen, Zhifeng Chen, Andy Davis, Jeffrey Dean, Matthieu Devin, Sanjay Ghemawat, Geoffrey Irving, Michael Isard, et al. Tensorflow: A system for large-scale machine learning. In *12th {USENIX} Symposium on Operating Systems Design and Implementation ({OSDI} 16)*, pages 265–283, 2016.
- [2] Guillaume Alain and Yoshua Bengio. Understanding intermediate layers using linear classifier probes. *arXiv preprint arXiv:1610.01644*, 2016.
- [3] Rahaf Aljundi, Francesca Babiloni, Mohamed Elhoseiny, Marcus Rohrbach, and Tinne Tuytelaars. Memory aware synapses: Learning what (not) to forget. In *Proceedings of the European Conference on Computer Vision (ECCV)*, pages 139–154, 2018.
- [4] Rahaf Aljundi, Klaas Kelchtermans, and Tinne Tuytelaars. Task-free continual learning. In *Proceedings of the IEEE Conference on Computer Vision and Pattern Recognition*, pages 11254–11263, 2019.
- [5] Rahaf Aljundi, Min Lin, Baptiste Goujaud, and Yoshua Bengio. Gradient based sample selection for online continual learning. In *Advances in Neural Information Processing Systems*, pages 11816–11825, 2019.
- [6] Arslan Chaudhry, Puneet K Dokania, Thalaiyasingam Ajanthan, and Philip HS Torr. Riemannian walk for incremental learning: Understanding forgetting and intransigence. In *Proceedings of the European Conference on Computer Vision (ECCV)*, pages 532–547, 2018.
- [7] Arslan Chaudhry, Marc’Aurelio Ranzato, Marcus Rohrbach, and Mohamed Elhoseiny. Efficient lifelong learning with a-gem. *arXiv preprint arXiv:1812.00420*, 2018.
- [8] Arslan Chaudhry, Marcus Rohrbach, Mohamed Elhoseiny, Thalaiyasingam Ajanthan, Puneet K Dokania, Philip HS Torr, and Marc’Aurelio Ranzato. Continual learning with tiny episodic memories. *arXiv preprint arXiv:1902.10486*, 2019.
- [9] Matthias De Lange, Rahaf Aljundi, Marc Masana, Sarah Parisot, Xu Jia, Ales Leonardis, Gregory Slabaugh, and Tinne Tuytelaars. Continual learning: A comparative study on how to defy forgetting in classification tasks. *arXiv preprint arXiv:1909.08383*, 2019.
- [10] Sebastian Farquhar and Yarin Gal. Towards robust evaluations of continual learning. *arXiv preprint arXiv:1805.09733*, 2018.
- [11] Chrisantha Fernando, Dylan Banarse, Charles Blundell, Yori Zwols, David Ha, Andrei A Rusu, Alexander Pritzel, and Daan Wierstra. Pathnet: Evolution channels gradient descent in super neural networks. *arXiv preprint arXiv:1701.08734*, 2017.
- [12] Robert M French. Catastrophic forgetting in connectionist networks. *Trends in cognitive sciences*, 3(4):128–135, 1999.
- [13] Xavier Glorot and Yoshua Bengio. Understanding the difficulty of training deep feedforward neural networks. In *Proceedings of the thirteenth international conference on artificial intelligence and statistics*, pages 249–256, 2010.
- [14] Siavash Golkar, Michael Kagan, and Kyunghyun Cho. Continual learning via neural pruning. *arXiv preprint arXiv:1903.04476*, 2019.
- [15] Ian J Goodfellow, Mehdi Mirza, Da Xiao, Aaron Courville, and Yoshua Bengio. An empirical investigation of catastrophic forgetting in gradient-based neural networks. *arXiv preprint arXiv:1312.6211*, 2013.
- [16] Yen-Chang Hsu, Yen-Cheng Liu, Anita Ramasamy, and Zsolt Kira. Re-evaluating continual learning scenarios: A categorization and case for strong baselines. *arXiv preprint arXiv:1810.12488*, 2018.
- [17] Ferenc Huszár. Note on the quadratic penalties in elastic weight consolidation. *Proceedings of the National Academy of Sciences*, page 201717042, 2018.

[18] Stanislaw Jastrzebski, Zachary Kenton, Nicolas Ballas, Asja Fischer, Yoshua Bengio, and Amos Storkey. On the relation between the sharpest directions of dnn loss and the sgd step length. *arXiv preprint arXiv:1807.05031*, 2018.

[19] Ronald Kemker and Christopher Kanan. Fearnnet: Brain-inspired model for incremental learning. *arXiv preprint arXiv:1711.10563*, 2017.

[20] Diederik P Kingma and Jimmy Ba. Adam: A method for stochastic optimization. *arXiv preprint arXiv:1412.6980*, 2014.

[21] James Kirkpatrick, Razvan Pascanu, Neil Rabinowitz, Joel Veness, Guillaume Desjardins, Andrei A Rusu, Kieran Milan, John Quan, Tiago Ramalho, Agnieszka Grabska-Barwinska, et al. Overcoming catastrophic forgetting in neural networks. *Proceedings of the national academy of sciences*, 114(13):3521–3526, 2017.

[22] Frederik Kunstner, Lukas Balles, and Philipp Hennig. Limitations of the empirical fisher approximation. *arXiv preprint arXiv:1905.12558*, 2019.

[23] Janice Lan, Rosanne Liu, Hattie Zhou, and Jason Yosinski. Lca: Loss change allocation for neural network training. In *Advances in Neural Information Processing Systems*, pages 3614–3624, 2019.

[24] Soochan Lee, Junsoo Ha, Dongsu Zhang, and Gunhee Kim. A neural dirichlet process mixture model for task-free continual learning. *arXiv preprint arXiv:2001.00689*, 2020.

[25] Xilai Li, Yingbo Zhou, Tianfu Wu, Richard Socher, and Caiming Xiong. Learn to grow: A continual structure learning framework for overcoming catastrophic forgetting. *arXiv preprint arXiv:1904.00310*, 2019.

[26] David Lopez-Paz and Marc’Aurelio Ranzato. Gradient episodic memory for continual learning. In *Advances in Neural Information Processing Systems*, pages 6467–6476, 2017.

[27] James Martens. New insights and perspectives on the natural gradient method. *arXiv preprint arXiv:1412.1193*, 2014.

[28] Michael McCloskey and Neal J. Cohen. Catastrophic interference in connectionist networks: The sequential learning problem. *Psychology of Learning and Motivation - Advances in Research and Theory*, 24(C):109–165, January 1989. ISSN 0079-7421. doi: 10.1016/S0079-7421(08)60536-8.

[29] Cuong V Nguyen, Yingzhen Li, Thang D Bui, and Richard E Turner. Variational continual learning. *arXiv preprint arXiv:1710.10628*, 2017.

[30] German I Parisi, Ronald Kemker, Jose L Part, Christopher Kanan, and Stefan Wermter. Continual lifelong learning with neural networks: A review. *Neural Networks*, 2019.

[31] Razvan Pascanu and Yoshua Bengio. Revisiting natural gradient for deep networks. *arXiv preprint arXiv:1301.3584*, 2013.

[32] Maithra Raghu, Justin Gilmer, Jason Yosinski, and Jascha Sohl-Dickstein. Svcca: Singular vector canonical correlation analysis for deep learning dynamics and interpretability. In *Advances in Neural Information Processing Systems*, pages 6076–6085, 2017.

[33] Dushyant Rao, Francesco Visin, Andrei Rusu, Razvan Pascanu, Yee Whye Teh, and Raia Hadsell. Continual unsupervised representation learning. In *Advances in Neural Information Processing Systems*, pages 7645–7655, 2019.

[34] Roger Ratcliff. Connectionist models of recognition memory: constraints imposed by learning and forgetting functions. *Psychological review*, 97(2):285, 1990.

[35] Sylvestre-Alvise Rebuffi, Alexander Kolesnikov, Georg Sperl, and Christoph H Lampert. icarl: Incremental classifier and representation learning. In *Proceedings of the IEEE conference on Computer Vision and Pattern Recognition*, pages 2001–2010, 2017.

- [36] Hippolyt Ritter, Aleksandar Botev, and David Barber. Online structured laplace approximations for overcoming catastrophic forgetting. In *Advances in Neural Information Processing Systems*, pages 3738–3748, 2018.
- [37] Jonathan Schwarz, Jelena Luketina, Wojciech M Czarnecki, Agnieszka Grabska-Barwinska, Yee Whye Teh, Razvan Pascanu, and Raia Hadsell. Progress & compress: A scalable framework for continual learning. *arXiv preprint arXiv:1805.06370*, 2018.
- [38] Hanul Shin, Jung Kwon Lee, Jaehong Kim, and Jiwon Kim. Continual learning with deep generative replay. In *Advances in Neural Information Processing Systems*, pages 2990–2999, 2017.
- [39] Ravid Shwartz-Ziv and Naftali Tishby. Opening the black box of deep neural networks via information. *arXiv preprint arXiv:1703.00810*, 2017.
- [40] Nitish Srivastava, Geoffrey Hinton, Alex Krizhevsky, Ilya Sutskever, and Ruslan Salakhutdinov. Dropout: a simple way to prevent neural networks from overfitting. *The journal of machine learning research*, 15(1):1929–1958, 2014.
- [41] Rupesh K Srivastava, Jonathan Masci, Sohrob Kazerounian, Faustino Gomez, and Jürgen Schmidhuber. Compete to compute. In C. J. C. Burges, L. Bottou, M. Welling, Z. Ghahramani, and K. Q. Weinberger, editors, *Advances in Neural Information Processing Systems 26*, pages 2310–2318. Curran Associates, Inc., 2013. URL <http://papers.nips.cc/paper/5059-compete-to-compute.pdf>.
- [42] Siddharth Swaroop, Cuong V Nguyen, Thang D Bui, and Richard E Turner. Improving and understanding variational continual learning. *arXiv preprint arXiv:1905.02099*, 2019.
- [43] Gido M van de Ven and Andreas S Tolias. Three scenarios for continual learning. *arXiv preprint arXiv:1904.07734*, 2019.
- [44] Friedemann Zenke, Ben Poole, and Surya Ganguli. Continual learning through synaptic intelligence. In *Proceedings of the 34th International Conference on Machine Learning-Volume 70*, pages 3987–3995. JMLR. org, 2017.